

# Fluid Bounding Effect on Natural Frequencies of Fluid-Coupled Circular Plates

**Myung Jo Jhung\***, **Young Hwan Choi**

*Korea Institute of Nuclear Safety,  
19 Guseong-dong, Yuseong-gu, Daejeon 305-338, Korea*

**Kyeong Hoon Jeong**

*Korea Atomic Energy Research Institute,  
150 Dukjin-dong, Yuseong-gu, Daejeon 305-353, Korea*

This study deals with the free vibration of two identical circular plates coupled with a bounded or unbounded fluid. An analytical method based on the finite Fourier-Bessel series expansion and Rayleigh-Ritz method is suggested. The proposed method is verified by the finite element analysis using commercial program with a good accuracy. The case of bounded or unbounded fluid is studied for the effect on the vibration characteristics of two circular plates. Also, the effect of gap between the plates on the fluid-coupled natural frequencies is investigated.

**Key Words :** Circular Plate, Fourier-Bessel Series, Rayleigh-Ritz Method, Fluid-Coupled System, In-Phase, Out-of-Phase, Normalized Frequency

## 1. Introduction

It is generally known that the natural frequencies of structures in contact with fluid, or immersed in fluid, decrease significantly compared to the natural frequencies in a vacuum. This problem is referred to as the fluid-structure interaction problem. For this problem, many investigators have obtained some approximate solutions that have been used to predict the changes in the natural frequencies of a structure in fluid. In recent literature, there has been renewed interest in the problem of plates vibrating in contact with water. This is stimulated by new technical applications and also by the availability of powerful numerical tools based on the finite element and boundary element methods which make numerical solutions of fluid-structure interaction problems possible.

However, the use of the finite element method or the boundary element method requires enormous amounts of time for modeling and computation.

Circular plates vibrating in contact with fluid have recently been studied. Kwak (1991) and Kwak and Kim (1991) studied the free vibrations of circular plates in contact with water on one side, while the free vibrations of annular plates in contact with water on one side were investigated by Amabili et al. (1996). They considered the unbounded fluid domain and also introduced the non-dimensionalized added virtual mass incremental factors in order to estimate the fluid effect on the individual natural frequency of the fluid-structure system. Chiba (1994) obtained exact solutions for the circular elastic bottom plate in a cylindrical rigid tank filled with fluid. The circular elastic bottom plate was supported by an elastic foundation and the free surface of the fluid was considered. Bauer (1995) analytically determined the coupled natural frequencies of an ideal fluid in a circular cylindrical container where the free fluid surface was covered by a flexible membrane cover or elastic plate. A paper by De Santo (1981) dealt with an experimental investigation

\* Corresponding Author,

E-mail : mjj@kins.re.kr

TEL : +82-42-868-0467; FAX : +82-42-868-0457

Korea Institute of Nuclear Safety, 19 Guseong-dong,  
Yuseong-gu, Daejeon 305-338, Korea. (Manuscript

Received January 17, 2003; Revised June 23, 2003)

of perforated circular plates submerged in water. Montero de Espinosa et al. (1984) studied the vibration of plates submerged in water mainly to the lower modes by the approximate analytical method and experiments. Hagedorn (1994) dealt with the theoretical free vibrations of an infinite elastic plate in the presence of water.

This study is concerned with the coupling effect of contacting fluid on the free vibration characteristics of circular plates coupled with incompressible and frictionless fluid. The natural frequencies of the in-phase and out-of-phase vibration modes of the fluid-coupled system could be obtained by theoretical calculations and the finite element method. The normalized natural frequencies are obtained in order to estimate the relative added mass effect of fluid on each vibration mode of the plates. The case of bounded or unbounded fluid is studied for the effect on the vibration characteristics of two circular plates. Also, the effect of contained fluid between plates on the frequencies is investigated by comparing frequencies according to the distance between plates.

## 2. Theoretical Development

### 2.1 Formulation

Figure 1 represents two identical circular plates coupled with fluid, where  $R$ ,  $h$  and  $H$  represent the radius and thickness of the plate, and distance between two plates respectively. The following assumptions are made for the theoretical development :

(a) the fluid motion is so small that it is considered to be linear,

(b) the fluid motion is incompressible, inviscid and irrotational,

(c) the material of plates is linearly elastic, homogeneous and isotropic.

The equation of motion for transverse displacement,  $w_j$ , of these plates which are in contact with fluid is :

$$D\nabla^4 w_j + \rho h w_{j,tt} = p_j, \quad j=1, 2 \quad (1)$$

where  $D = Eh^3/12(1-\mu^2)$  is the flexural rigidity of the plates ;  $\rho$ ,  $\mu$ ,  $p_j$  and  $E$  are density, Poisson's ratio, hydrodynamic pressure on the plates and Young's modulus of the plates, respectively. The upper circular plate is referred to with a subscript "1" while the lower circular plate is denoted by a subscript "2." The solution of Eq. (1) takes the following form of combinations for plate deformation with respect to polar coordinates  $(r, \theta)$  :

$$w_1(r, \theta, t) = \cos(n\theta) \sum_{m=1}^M q_m W_{nm1}(r) \exp(i\omega t) \quad (2a)$$

$$w_2(r, \theta, t) = \cos(n\theta) \sum_{m=1}^M q_m W_{nm2}(r) \exp(i\omega t) \quad (2b)$$

where  $q_m$  and  $p_m$  are unknown coefficients and  $n$  and  $m$  are the numbers of the nodal diameters and circles of the plates, respectively. For the plate with clamped boundary conditions, the displacement along the edge of the plates must be zero and therefore dynamic displacement of Eq. (2) will be reduced to :

$$W_{nmj}(r) = J_n(\lambda_{nm}r) - J_n(\lambda_{nm}R) \frac{I_n(\lambda_{nm}r)}{I_n(\lambda_{nm}R)}, \quad j=1, 2 \quad (3)$$

where  $\lambda_{nm}$  is the frequency parameter for the disks, which is also determined by the boundary conditions and is related to the circular frequency  $\omega$ .  $J_n$  and  $I_n$  are the Bessel function and the modified Bessel function of the first kind, respectively. For the fixed boundary condition, the eigenvalues  $\lambda_{nm}$  for the plate in a vacuum can be obtained from the zero slope and zero moment boundary conditions as follows (Bauer, 1995) :

$$J_n(\lambda_{nm}R) I_{n+1}(\lambda_{nm}R) + J_{n+1}(\lambda_{nm}R) I_n(\lambda_{nm}R) = 0 \quad (4)$$

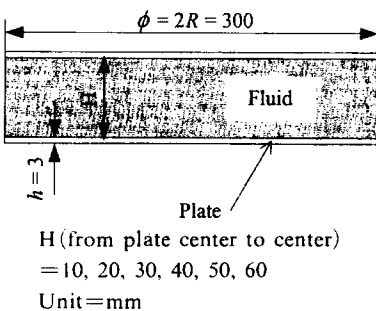


Fig. 1 Two plates coupled with fluid

**2.2 Velocity potential**

Let's consider the fluid region between the circular plates. The three-dimensional oscillatory fluid flow in the cylindrical coordinates can be described by the velocity potential. The facing side of the plates is in contact with inviscid and incompressible fluid. The fluid movement due to the plate vibration is described by the spatial velocity potential that satisfies the equation :

$$\nabla^2 \Phi(x, r, \theta, t) = 0 \tag{5}$$

It is possible to separate the function  $\Phi$  with respect to  $r$  by observing that in the radial direction the vessel which supports the edges of the plates are assumed to be rigid, as in the case of the completely contact circular plate. Thus :

$$\Phi(x, r, \theta, t) = i\omega\phi(r, \theta, x)\exp(i\omega t) \tag{6}$$

Substituting Eq. (6) into Eq. (5) generates the general solution of Eq. (5) as :

$$\phi(r, \theta, x) = \sum_{s=1}^{\infty} [J_n(\beta_{ns}r) \{ E_{ns} \sinh(\beta_{ns}x) + F_{ns} \cosh(\beta_{ns}x) \}] \cos(n\theta) \tag{7}$$

For the bounded fluid, the boundary condition along the cylindrical vessel wall assures the zero fluid velocity given by :

$$\partial\phi/\partial r|_{r=R} = 0 \tag{8}$$

Insertion of Eq. (7) into Eq. (8) determines  $\beta_{ns}$  for every  $n$  and  $s$  by the equation :

$$J_n'(\beta_{ns}R) = 0 \tag{9}$$

On the other hand, the coefficients  $\beta_{ns}$  for the unbounded fluid can be determined by the following transcendental equation with respect to every  $n$  and  $s$  :

$$J_n(\beta_{ns}R) = 0 \tag{10}$$

where Eq. (10) satisfies the fluid boundary condition of the free surface, which means zero velocity potential at  $r=R$  :

$$\phi(r, \theta, x) = 0 \text{ at } r=R \tag{11}$$

When we consider the symmetry of the fluid velocities for the in-phase and out-of-phase vibration modes, the velocity potential will require the following symmetric conditions :

for the in-phase mode,

$$\partial\phi(r, \theta, -x)/\partial x = \partial\phi(r, \theta, x)/\partial x \tag{12}$$

and for the out-of-phase mode,

$$\partial\phi(r, \theta, x)/\partial x|_{x=0} = 0 \tag{13}$$

Application of Eqs. (12) and (13) gives simple reduced forms of Eq. (7) :

for the in-phase mode,

$$\begin{aligned} \phi(r, \theta, x) &= \cos(n\theta) \sum_{s=1}^{\infty} E_{ns} J_n(\beta_{ns}r) \sinh(\beta_{ns}x) \\ &= \cos(n\theta) \phi_1(r, x) \end{aligned} \tag{14}$$

and for the out-of-phase mode,

$$\begin{aligned} \phi(r, \theta, x) &= \cos(n\theta) \sum_{s=1}^{\infty} F_{ns} J_n(\beta_{ns}r) \cosh(\beta_{ns}x) \\ &= \cos(n\theta) \phi_2(r, x) \end{aligned} \tag{15}$$

**2.3 Method of solution**

In order to determine the coefficients  $E_{ns}$  and  $F_{ns}$  of fluid motion, the compatibility conditions at the interface of the upper and lower fluid domains contacting along the plate surfaces are used. Compatibility conditions at the fluid interface with the plates yield

$$w_1 = -\partial\phi/\partial x|_{x=H/2} \tag{16}$$

$$w_2 = -\partial\phi/\partial x|_{x=-H/2} \tag{17}$$

Substitution of Eqs. (2), (3), (14) and (15) into Eqs. (16) and (17) gives :

For the in-phase mode,

$$\begin{aligned} \sum_{m=1}^M q_m \left[ J_n(\lambda_{nm}r) - J_n(\lambda_{nm}R) \frac{I_n(\lambda_{nm}r)}{I_n(\lambda_{nm}R)} \right] \\ = - \sum_{s=1}^{\infty} E_{ns} \beta_{ns} J_n(a_{ns}r) \cosh\left(\beta_{ns} \frac{H}{2}\right) \end{aligned} \tag{18}$$

and for the out-of-phase mode,

$$\begin{aligned} \sum_{m=1}^M q_m \left[ J_n(\lambda_{nm}r) - J_n(\lambda_{nm}R) \frac{I_n(\lambda_{nm}r)}{I_n(\lambda_{nm}R)} \right] \\ = - \sum_{s=1}^{\infty} F_{ns} \beta_{ns} J_n(a_{ns}r) \cosh\left(\beta_{ns} \frac{H}{2}\right) \end{aligned} \tag{19}$$

Expanding  $J_n(\lambda_{nm}r)$  and  $I_n(\lambda_{nm}r)$  of Eqs. (18) and (19) into Bessel-Fourier series of the form (Hagedorn, 1994 ; Sneddon, 1951) will give :

$$J_n(\lambda_{nm}r) = \sum_{s=1}^{\infty} a_{nms} J_n(\beta_{ns}r) \tag{20a}$$

$$I_n(\lambda_{nm}r) = \sum_{s=1}^{\infty} b_{nms} J_n(\alpha_{ns}r) \tag{20b}$$

The Bessel-Fourier coefficients  $a_{nms}$  and  $b_{nms}$  can be written as Eq. (21a-d) for the bounded fluid case, where the coefficients  $\beta_{ns}$  must satisfy Eq. (9).

For  $n=0$ ,

$$a_{oms} = \frac{-2(\lambda_{om}R) J_1(\lambda_{om}R)}{[(\beta_{os}R)^2 - (\lambda_{om}R)^2] J_0(\beta_{os}R)} \tag{21a}$$

$$b_{oms} = \frac{2(\lambda_{om}R) I_1(\lambda_{om}R)}{[(\beta_{os}R)^2 + (\lambda_{om}R)^2] J_0(\beta_{os}R)} \tag{21b}$$

and for  $n > 0$

$$a_{nms} = \frac{2(\beta_{ns}R)^2(\lambda_{nm}R) J_n'(\lambda_{nm}R)}{[(\beta_{ns}R)^2 - n^2][(\beta_{ns}R)^2 - (\lambda_{nm}R)^2] J_n(\beta_{ns}R)} \tag{21c}$$

$$b_{nms} = \frac{2(\beta_{ns}R)^2(\lambda_{nm}R) I_n'(\lambda_{nm}R)}{[(\beta_{ns}R)^2 - n^2][(\beta_{ns}R)^2 + (\lambda_{nm}R)^2] J_n(\beta_{ns}R)} \tag{21b}$$

On the other hand, for the unbounded fluid case, the Bessel-Fourier coefficients  $a_{nms}$  and  $b_{nms}$  can be written as Eq. (22a, b), where the coefficients  $\beta_{ns}$  must satisfy Eq. (10) instead of Eq. (9).

$$a_{nms} = \frac{2(\beta_{ns}R) J_n(\lambda_{nm}R)}{[(\beta_{ns}R)^2 - (\lambda_{nm}R)^2] J_{n+1}(\beta_{ns}R)} \tag{22a}$$

$$b_{nms} = \frac{2(\beta_{ns}R) I_n(\lambda_{nm}R)}{[(\beta_{ns}R)^2 - (\lambda_{nm}R)^2] J_{n+1}(\beta_{ns}R)} \tag{22b}$$

Therefore, the velocity potential of the fluid can be written in terms of unknown constants  $q_m$  instead of the unknown coefficients  $E_{ns}$  or  $F_{ns}$ . For the in-phase modes,

$$\phi(r, \theta, x) = \sum_{m=1}^M q_m \sum_{s=1}^{\infty} \mathcal{E}_{nms} J_n(\beta_{ns}r) \sinh(\beta_{ns}x) \cos(n\theta) \tag{23a}$$

and for the out-of-phase modes,

$$\phi(r, \theta, x) = \sum_{m=1}^M q_m \sum_{s=1}^{\infty} \mathcal{E}_{nms} J_n(\beta_{ns}r) \cosh(\beta_{ns}x) \cos(n\theta) \tag{23b}$$

where  $\mathcal{E}_{nms}$  is a derived coefficient :

$$\mathcal{E}_{nms} = - \frac{[a_{nms} - b_{nms} J_n(\lambda_{nm}R) / I_n(\lambda_{nm}R)]}{\beta_{ns} \cosh(\beta_{ns}H/2)} \tag{24a}$$

for the in-phase modes

$$\mathcal{E}_{nms} = - \frac{[a_{nms} - b_{nms} J_n(\lambda_{nm}R) / I_n(\lambda_{nm}R)]}{\beta_{ns} \sinh(\beta_{ns}H/2)} \tag{24b}$$

for the out-of-phase modes

In order to perform numerical calculations for each fixed  $n$  value, a sufficiently large finite enough number  $M$  of terms must be considered in all the previous sums of the expanding term,  $m$ . For this purpose, a vector  $\mathbf{q}$  of the unknown parameters is introduced as :

$$\mathbf{q} = \{ q_1 \ q_2 \ q_3 \ \dots \ q_M \}^T \tag{25}$$

Now, it is necessary to know the reference kinetic energies of the plates and containing fluid in order to calculate the coupled natural frequencies of the circular plates in contact with fluid. The reference kinetic energy of the fluid can be evaluated as :

$$T_F = -\frac{1}{2} \rho_o \kappa_{\theta} \left[ \int_0^R w_1 \phi_j \left( r, \frac{H}{2} \right) r dr + \int_0^R w_2 \phi_j \left( r, -\frac{H}{2} \right) r dr \right], \quad j=1, 2 \tag{26}$$

where  $\kappa_{\theta} = 2\pi$  for  $n=0$  and  $\kappa_{\theta} = \pi$  for  $n > 0$ . Insertion of Eqs. (3) and (23a, b) into Eq. (26) gives the reference kinetic energy of the fluid :

$$T_F = \rho_o \kappa_{\theta} \mathbf{q}^T \mathbf{G} \mathbf{q} \tag{27}$$

where  $\rho_o$  is the mass density of the fluid, and the  $M \times M$  symmetric matrix  $\mathbf{G}$  for the fixed  $n$  is given by Eqs. (20a, b), (21a-d) and (26) as follows and they are called added virtual mass incremental (AVMI) matrix (Kwak and Kim, 1991 ; Chiba, 1994).

For the fixed boundary condition of the plates and bounded fluid case,

$$G_{ik} = - \sum_{s=1}^{\infty} \frac{8R^3(\beta_{ns}R) A_{is} A_{ks} B_{ns}}{[(\beta_{ns}R)^2 - n^2]}, \quad i, k=1, 2, \dots, M \tag{28}$$

with

$$A_{is} = \frac{(\lambda_{ni}R)^3 J_n'(\lambda_{ni}R)}{[(\beta_{ns}R)^4 - (\lambda_{ni}R)^4]} \tag{29a}$$

$$A_{ks} = \frac{(\lambda_{nk}R)^3 J_n'(\lambda_{nk}R)}{[(\beta_{ns}R)^4 - (\lambda_{nk}R)^4]} \tag{29b}$$

$$\beta_{ns} = \tanh \left( \beta_{ns} \frac{H}{2} \right), \tag{30a}$$

for the in-phase mode

$$\beta_{ns} = \coth \left( \beta_{ns} \frac{H}{2} \right), \tag{30b}$$

for the out-of-phase mode

When the plates have a fixed boundary condition and the fluid is unbounded, the AVMI matrix will be reduced to

$$G_{ik} = \sum_{s=1}^{\infty} \frac{8R^3(\beta_{ns}R)(\lambda_{ni}R)^2(\lambda_{nk}R)^2 J_n(\lambda_{ni}R) J_n(\lambda_{nk}R)}{[(\lambda_{ni}R)^4 - (\beta_{ns}R)^4][(\lambda_{nk}R)^4 - (\beta_{ns}R)^4]} \beta_{ns}, \quad (31)$$

$i, k=1, 2, \dots, M$

The sum on  $s$  in Eqs. (28) and (31) must be stopped for numerical computation, at an integer value large enough to give the required accuracy. For the fluid bounded case with  $n=0$  and  $s=1$ , the first term of  $G_{ik}$  has a zero denominator and a zero numerator at the same time for the in-phase modes because of  $\beta_{ns}=0$ . The limit of the first term of  $G_{ik}$  must be determined as  $\beta_{ns}$  approaches zero. In consequence of formulation, the first term of  $G_{ik}$  for the in-phase modes with  $n=0$  will be replaced with  $4HR^2 J_1(\lambda_{0i}R) J_1(\lambda_{0k}R) / [(\lambda_{0i}R)(\lambda_{0k}R)]$  instead of the first term of Eq. (28). On the other hand, For the fluid unbounded case with  $n=0$  and  $s=1$ , the first term of  $G_{ik}$  for the out-of-phase modes must be replaced with  $8R^4 J_1(\lambda_{0k}R) J_0(\lambda_{0i}R) / [(\lambda_{0i}R)^2(\lambda_{0k}R)H]$  instead of the first term of Eq. (31).

The reference kinetic energy of the two circular plates, as obtained using the orthogonality of the mode shapes, is presented :

$$T_d = \rho h \kappa_0 \int_0^R w_1^2 r dr \quad (32)$$

Insertion of Eq. (2) into Eq. (32) gives the kinetic energy of the two circular plates as :

$$T_d = \rho h \kappa_0 \mathbf{q}^T \mathbf{Z} \mathbf{q} \quad (33)$$

where  $\mathbf{Z}$  is  $M \times M$  matrix given as

$$Z_{ik} = \delta_{ik} \int_0^R r W_{ni} W_{nk} r dr, \quad (34)$$

$\delta_{ik}$  : Kronecker delta

When Eq. (3) is inserted into Eq. (34) and the integration is carried out, matrix  $\mathbf{Z}$  is simply represented as :

$$Z_{ik} = R^2 \{ J_n(\lambda_{ni}R) \}^2 \delta_{ik} \quad (35)$$

The maximum potential energy of the two plates can be computed as :

$$V_d = \kappa_0 D \int_0^R \left( [\nabla^2 w_1]^2 - 2(1-\mu) \left\{ \frac{\partial^2 w_1}{\partial r^2} \left( \frac{1}{r} \frac{\partial w_1}{\partial r} + \frac{1}{r^2} \frac{\partial^2 w_1}{\partial \theta^2} \right) - \left( \frac{\partial}{\partial r} \left[ \frac{1}{r} \frac{\partial w_1}{\partial \theta} \right] \right)^2 \right\} \right) r dr \quad (36)$$

As the first term  $[\nabla^2 w_1]^2$  of Eq. (36) is identical to  $\lambda_{ni}^4 w_1^2$  and the other terms of Eq. (36) are negligible comparing with the first term, the maximum potential energy may be approximated by

$$V_d \approx \kappa_0 D \mathbf{q}^T \mathbf{P} \mathbf{q} \quad (37)$$

where  $\mathbf{P}$  is the  $M \times M$  diagonal matrix given by

$$P_{ik} = \frac{(\lambda_{ni}R)^4}{R^2} \{ J_n(\lambda_{ni}R) \}^2 \delta_{ik} \quad (38)$$

The correspondence between the reference total kinetic energy of each mode multiplied by its square circular frequency and the maximum potential energy of the same mode are used. In order to find the coupled natural frequencies and mode shapes of the two plates in contact with fluid, the Rayleigh quotient for the plates vibration coupled with ideal fluid is used. Minimizing Rayleigh quotient  $V_d / (T_d + T_F)$  with respect to the unknown parameters  $q_m$ , the non-dimensional Galerkin equation can be obtained :

$$D \mathbf{P} \mathbf{q} - \omega^2 (\rho h \mathbf{Z} + \rho_o \mathbf{G}) \mathbf{q} = \{ 0 \} \quad (39)$$

Eq. (39) gives an eigenvalue problem and the coupled natural frequency  $\omega$  can be calculated.

### 3. Analysis

#### 3.1 Theoretical analysis

On the basis of the preceding analysis, the determinant of the left side in Eq. (39) is numerically solved using MathCAD for the clamped edge condition in order to find the coupled natural frequencies of two circular plates coupled with fluid. In order to check the validity and accuracy of the results from the theoretical study, finite element analyses are also performed and frequency comparisons between them are carried out for the fluid-coupled system.

The circular plates are made of aluminum having a mean radius of 150 mm and a thickness of 3 mm. Also the distance between two plates

**Table 1** Dimensions and material properties

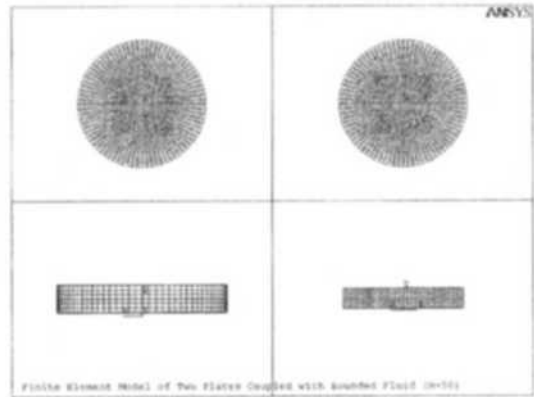
	Unit	Plate	Fluid
Young's modulus	Pa	69E9	
Poisson's ratio		0.3	
Density	kg/m <sup>3</sup>	2700	1000
Sound speed	m/sec		1483
Bulk modulus of elasticity	Pa		2.2E9
Thickness	mm	3	
Diameter	mm	300	

are varied from 10 mm to 60 mm to see the effect of the quantity of contained fluid on the modal characteristics of the plates (Fig. 1). The physical properties of the material are as follows: Young's modulus=69.0 GPa, Poisson's ratio=0.3, and mass density=2700 kg/m<sup>3</sup>. Water is used as the contained fluid, having a density of 1000 kg/m<sup>3</sup>. The sound speed in water is 1483 m/s, which is equivalent to the bulk modulus of elasticity of 2.2 GPa (Table 1). The clamped edge condition of the plates is considered among the possible boundary conditions.

The frequency equations derived in the preceding sections involve an infinite series of algebraic terms. Before exploring the analytical method to obtain the natural frequencies of the fluid-coupled plates, it is necessary to conduct convergence studies and establish the number of terms required in the series expansions involved. In the numerical calculation, the Bessel-Fourier expansion term  $s$  is set to 200 and the expanding term  $m$  (or  $M$ ) for the admissible function is set to 40, which gives an exact enough solution by convergence. In general, the solution approaches the exact frequency from above as the number of terms included in the series Eqs. (27), (33) and (37) increases, which may increase the calculation time significantly.

### 3.2 Finite element analysis

Finite element analyses using a commercial computer code ANSYS 6.1 (ANSYS 2001) are performed to verify the analytical results for the theoretical study. The results from finite element method are used as the baseline data. Three-

**Fig. 2** Finite element model of two plates coupled with fluid

dimensional model is constructed for the finite element analysis. The fluid region is divided into a number of 3-dimensional contained fluid elements (FLUID80) with eight nodes having three degrees of freedom at each node. The fluid element FLUID80 is particularly well suited for calculating hydrostatic pressures and fluid/solid interactions. The circular plates are modeled as elastic shell elements (SHELL63) with four nodes. The model for  $H=50$  mm has 7200 fluid elements and 2400 shell elements as shown in Fig. 2.

The boundary conditions at the plate perimeter nodes are fixed. The fluid movement at  $r=R$  is considered to be constrained in the radial direction for the bounded fluid case but no constraints are imposed for the unbounded fluid case. The vertical velocities of the fluid element nodes adjacent to each surface of the wetted circular plates coincide to those of plates so that the model can simulate Eqs. (16) and (17).

The Block Lanczos method is used for the eigenvalue and eigenvector extractions to calculate 400 frequencies, which are composed of in-phase and out-of-phase modes.

## 4. Results and Discussion

Mode shapes ( $m'=1$ ) of in-phase and out-of-phase from finite element analysis for fixed plates with unbounded fluid of  $H=50$  mm are shown in Fig. 3. For identical modes in the radial direction, in-phase and out-of-phase modes appear

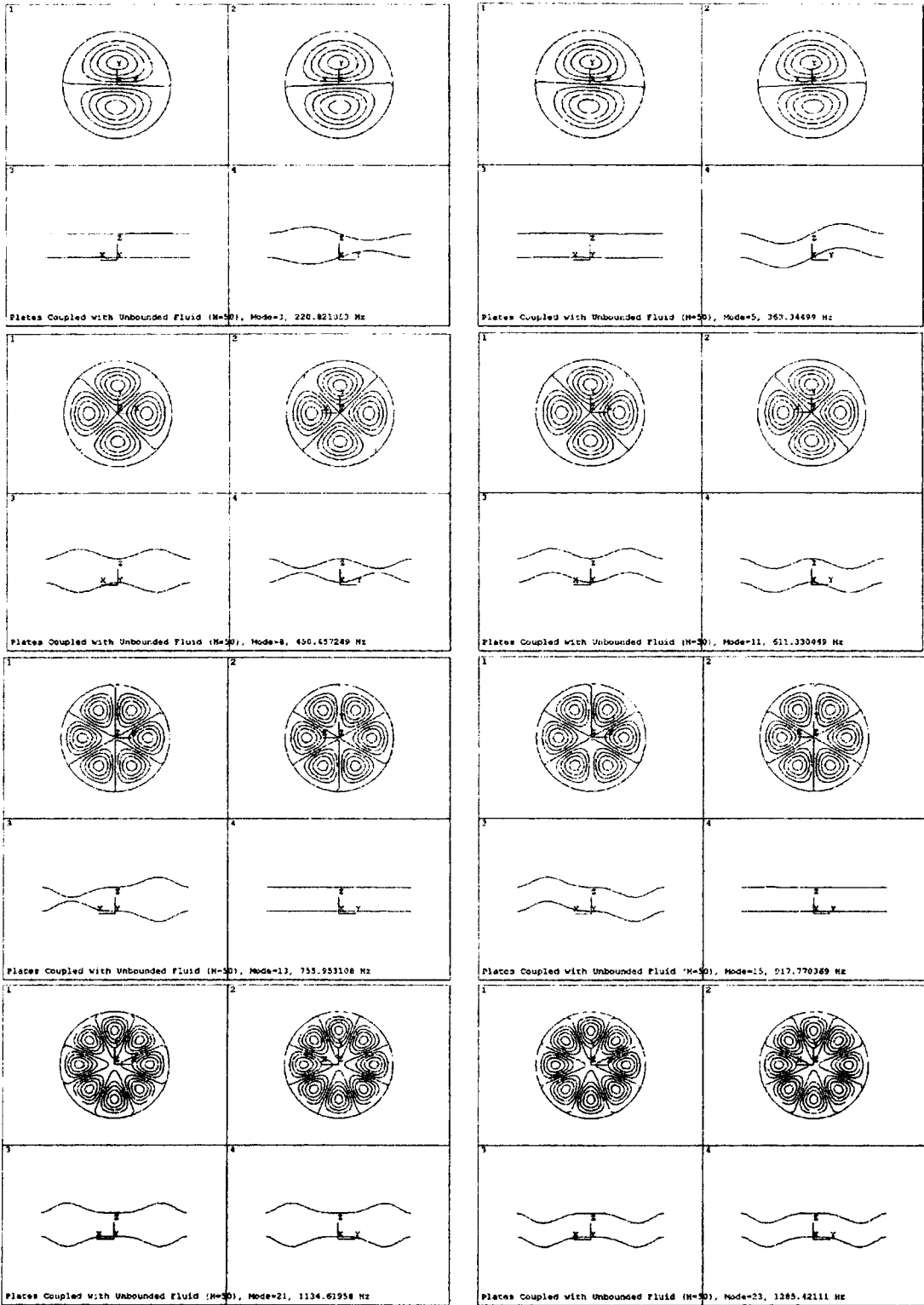


Fig. 3 Mode shapes of two plates for  $m'=1$

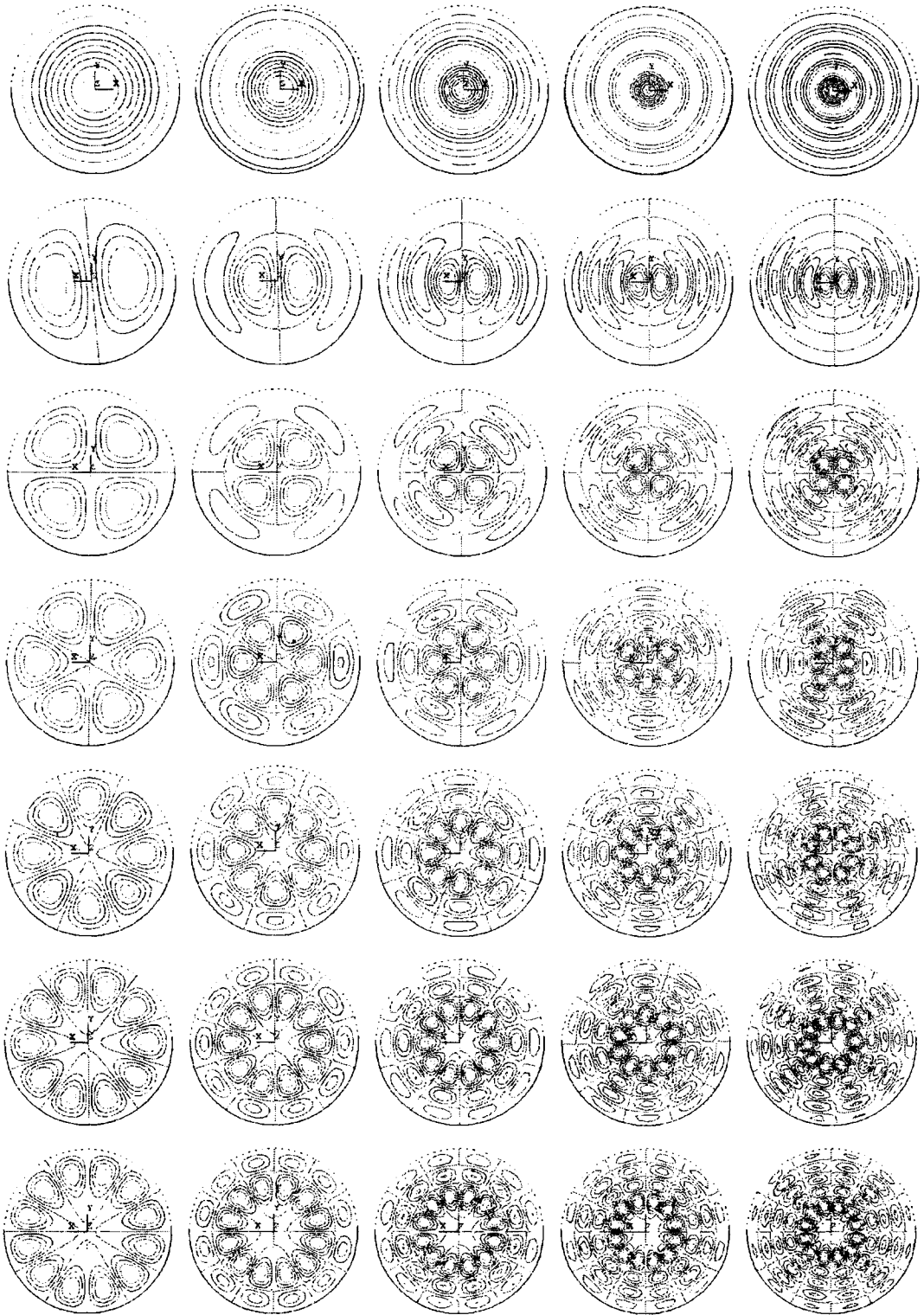


Fig. 4 Typical mode shapes of plate for radial mode



**Table 2** Comparison of in-phase mode frequencies between FEM and theory for plates coupled with bounded fluid

$n$	$m'=1$			$m'=2$			$m'=3$		
	FEM	Theory	Disc. (%)	FEM	Theory	Disc. (%)	FEM	Theory	Disc. (%)
0	171	168	1.8	700	695	0.7	1666	1678	-0.7
1	363	358	1.4	1102	1102	0.0	2310	2343	-1.4
2	609	605	0.7	1574	1586	-0.8	3034	3099	-2.1
3	914	913	0.1	2121	2151	-1.4	3838	3946	-2.8
4	1279	1285	-0.5	2741	2798	-2.1	4720	4884	-3.5
5	1706	1724	-1.1	3432	3527	-2.8	5677	5913	-4.2
6	2198	2233	-1.6	4197	4338	-3.4	6707	7030	-4.8

**Table 3** Comparison of out-of-phase mode frequencies between FEM and theory for plates coupled with bounded fluid

$n$	$m'=1$			$m'=2$			$m'=3$		
	FEM	Theory	Disc. (%)	FEM	Theory	Disc. (%)	FEM	Theory	Disc. (%)
0	—	—	—	405	391	3.5	1337	1385	-3.6
1	150	154	-2.7	791	813	-2.8	1995	2061	-3.3
2	371	381	-2.7	1282	1320	-3.0	2750	2853	-3.7
3	674	692	-2.7	1862	1920	-3.1	3591	3742	-4.2
4	1055	1081	-2.5	2519	2606	-3.5	4511	4721	-4.7
5	1507	1544	-2.5	3249	3371	-3.8	5503	5785	-5.1
6	2027	2079	-2.6	4050	4215	-4.1	6562	6931	-5.6

**Table 4** Comparison of in-phase mode frequencies between FEM and theory for plates coupled with unbounded fluid

$n$	$m'=1$			$m'=2$			$m'=3$		
	FEM	Theory	Disc. (%)	FEM	Theory	Disc. (%)	FEM	Theory	Disc. (%)
0	171	168	1.8	702	699	0.4	1682	1698	-1.0
1	363	359	1.1	1109	1112	-0.3	2337	2376	-1.7
2	611	608	0.5	1588	1603	-0.9	3074	3144	-2.3
3	918	919	-0.1	2142	2177	-1.6	3891	4004	-2.9
4	1286	1295	-0.7	2770	2832	-2.2	4786	4954	-3.5
5	1718	1739	-1.2	3470	3569	-2.9	5756	5992	-4.1
6	2214	2253	-1.8	4243	4388	-3.4	6798	7117	-4.5

**Table 5** Comparison of out-of-phase mode frequencies between FEM and theory for plates coupled with unbounded fluid

$n$	$m'=1$			$m'=2$			$m'=3$		
	FEM	Theory	Disc. (%)	FEM	Theory	Disc. (%)	FEM	Theory	Disc. (%)
0	71	73	-2.8	534	545	-2.1	1536	1568	-2.1
1	221	226	-2.3	944	964	-3.1	2217	2268	-2.3
2	450	460	-2.2	1442	1473	-2.1	2979	3059	-2.7
3	756	772	-2.1	2018	2067	-2.4	3818	3938	-3.1
4	1136	1160	-2.1	2669	2742	-2.7	4732	4903	-3.6
5	1584	1620	-2.3	3390	3498	-3.2	5716	5954	-4.2
6	2101	2151	-2.4	4181	4333	-3.6	6769	7089	-4.7

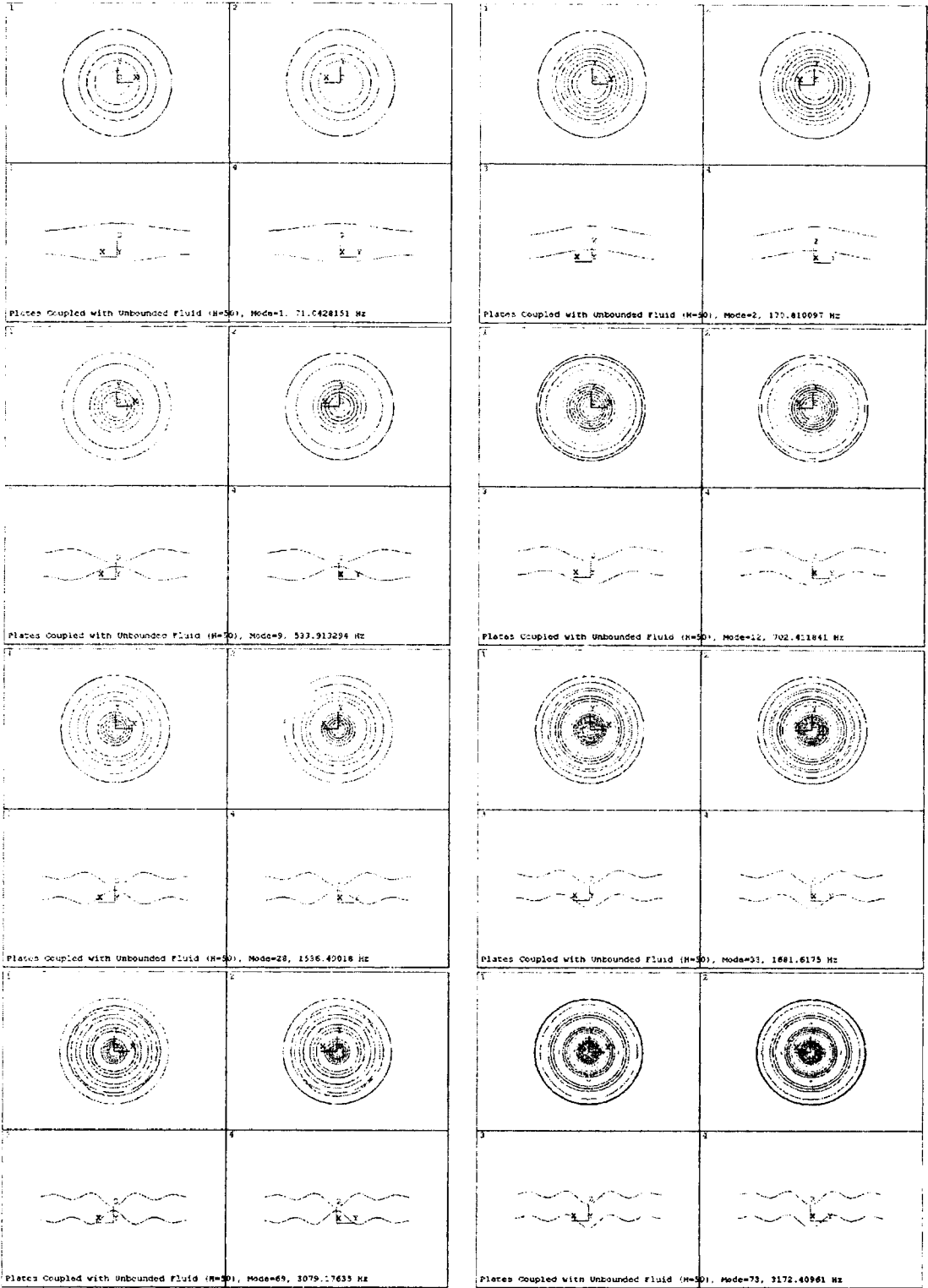


Fig. 5 Mode shapes of  $n=0$  for  $H=50$  mm

alternately and out-of phase modes are always shown ahead of in-phase modes. Fig. 4 shows the typical mode shapes of radial modes.

The frequency comparisons between analytical solution developed here and finite element method are shown in Tables 2 through 5 for  $H=50$  mm. The symbol  $m'$  in the tables represents the number of nodal circles of the wet mode and the symbol  $n$  means the number of nodal diameter. The discrepancy in the tables is defined by :

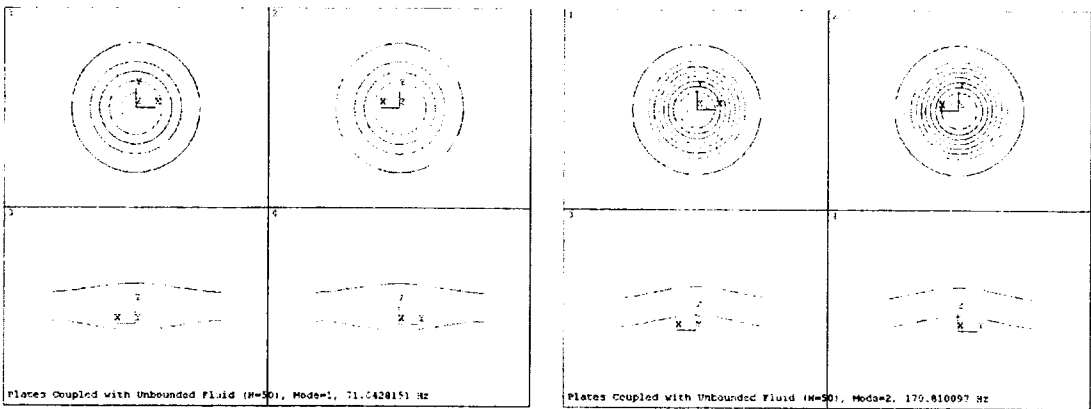
$$\text{Discrepancy}(\%) = \frac{\text{frequency by FEM} - \text{theoretical frequency}}{\text{frequency by FEM}} \times 100 \quad (40)$$

As shown in Tables 2 through 5, the largest discrepancy between the theoretical and finite element analysis results for fixed plates is 5.6% for the out-of-phase mode  $m'=3$  and  $n=6$  of

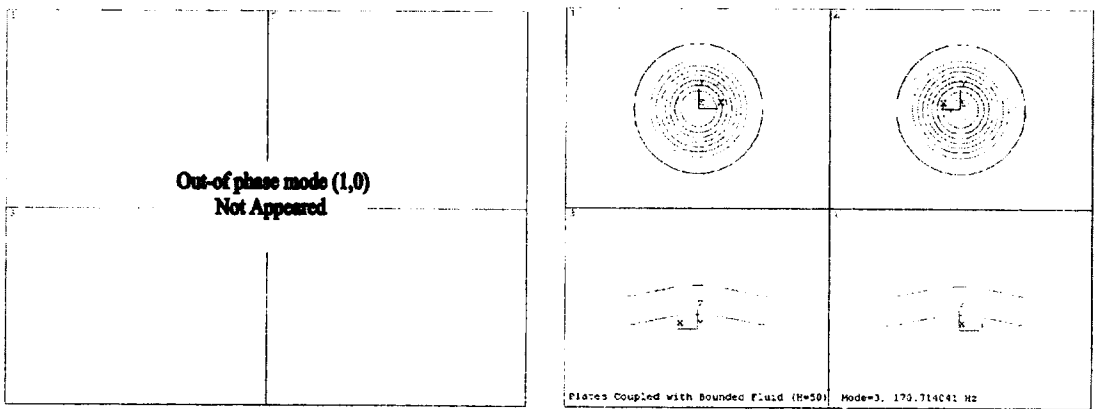
bounded fluid case. Therefore the theoretical results agree well with finite element analysis results, verifying the validity of the analytical method developed. Frequencies from finite element analysis are generally lower than those of theory due to the fact that the boundary conditions of plates are not simulated to be clamped perfectly.

Mode shapes of  $n=0$  are shown in Fig. 5, where the out-of-phase mode of unbounded fluid case for  $m'=1$  and  $n=0$  is shown but it does not appear in the bounded fluid case due to the restriction of the fluid volume conservation (Fig. 6).

Frequencies of plates coupled with unbounded fluid for the in-phase and out-of-phase modes are represented in Figs. 7 and 8 with respect to the distance between two plates. In all cases, as the number of nodal circles increases, frequency



(a) Unbounded case



(b) Bounded case

Fig. 6 Comparison of (1, 0) mode shapes between bounded and unbounded cases

increases, which were not shown in cylindrical shells (Jhung et al., 2002). Also, the frequencies of in-phase modes are always higher than those of corresponding out-of-phase modes and as mode number and the distance between two plates decrease the difference between in-phase and out-of-phase modes increases.

The effect of fluid on the frequencies of two circular plates wetted with fluid can be assessed

using the normalized frequency defined as :

$$\text{Normalized frequency} = \frac{\text{Frequency with fluid}}{\text{Frequency without fluid}} \quad (41)$$

The normalized natural frequencies for the in-phase and out-of-phase modes have values between one and zero due to the added mass effect of fluid. Figs. 9 and 10 show the normalized natural frequencies for in-phase and out-of-

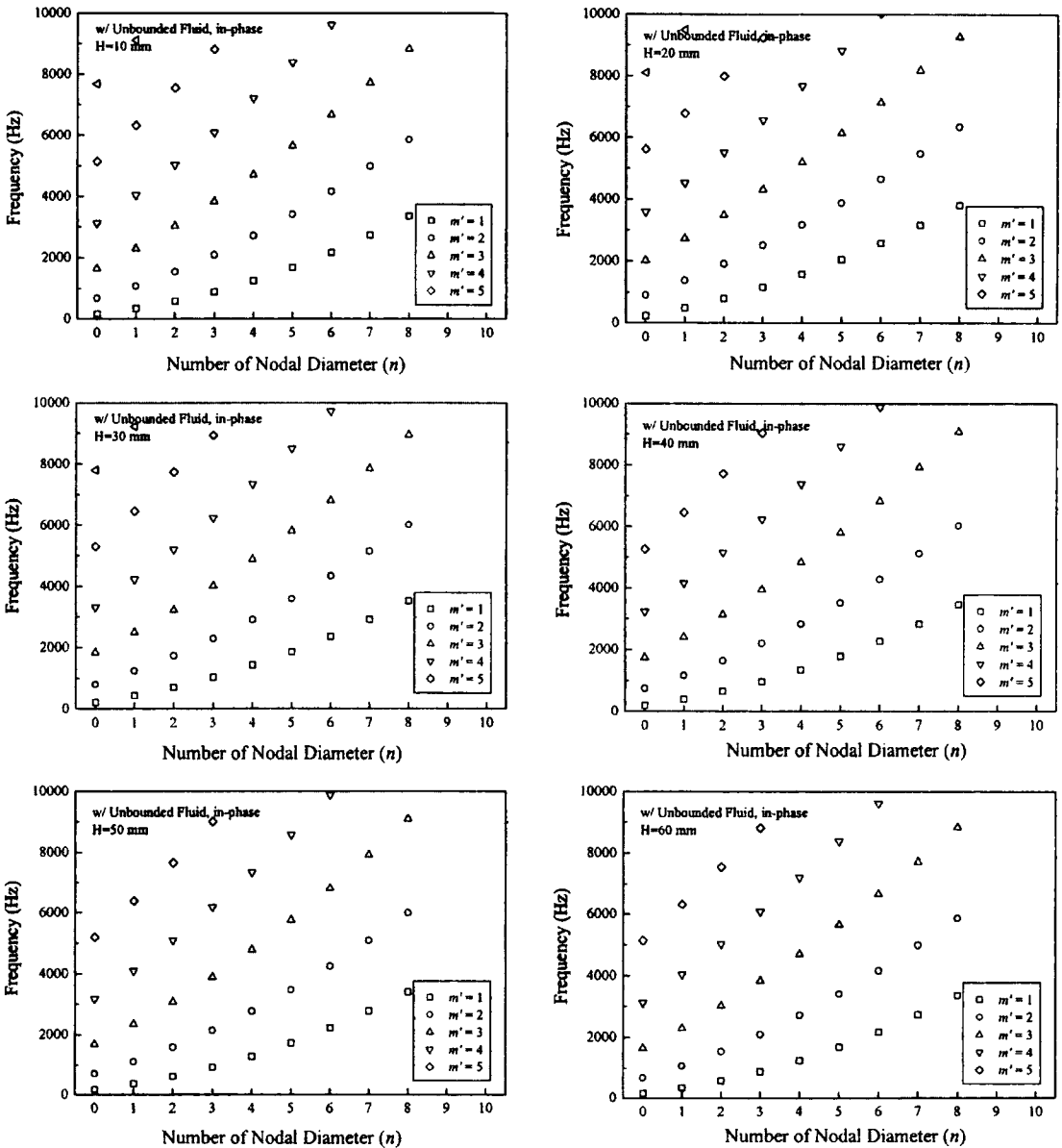


Fig. 7 In-phase mode frequencies of two plates coupled with fluid

phase modes, respectively. The fluid affects the out-of-phase mode more significantly than the in-phase mode. Especially the in-phase mode has the same effect irrespective of the number of nodal circles and nodal diameters but out-of-phase mode has more effect with the smaller number of nodal circles and nodal diameters. As the number of nodal circles or diameters of the plates increases, the normalized natural frequencies in-

crease by the gradual reduction of the relative added mass effect. Therefore, an increase of nodal lines or nodal circles causes an increase in the normalized natural frequencies for both in-phase and out-of-phase modes.

Figures 11 and 12 show fluid gap effect on the natural frequencies of in-phase and out-of-phase modes. As we compare the natural frequencies in Figs. 11 and 12, the decrease of the distance,

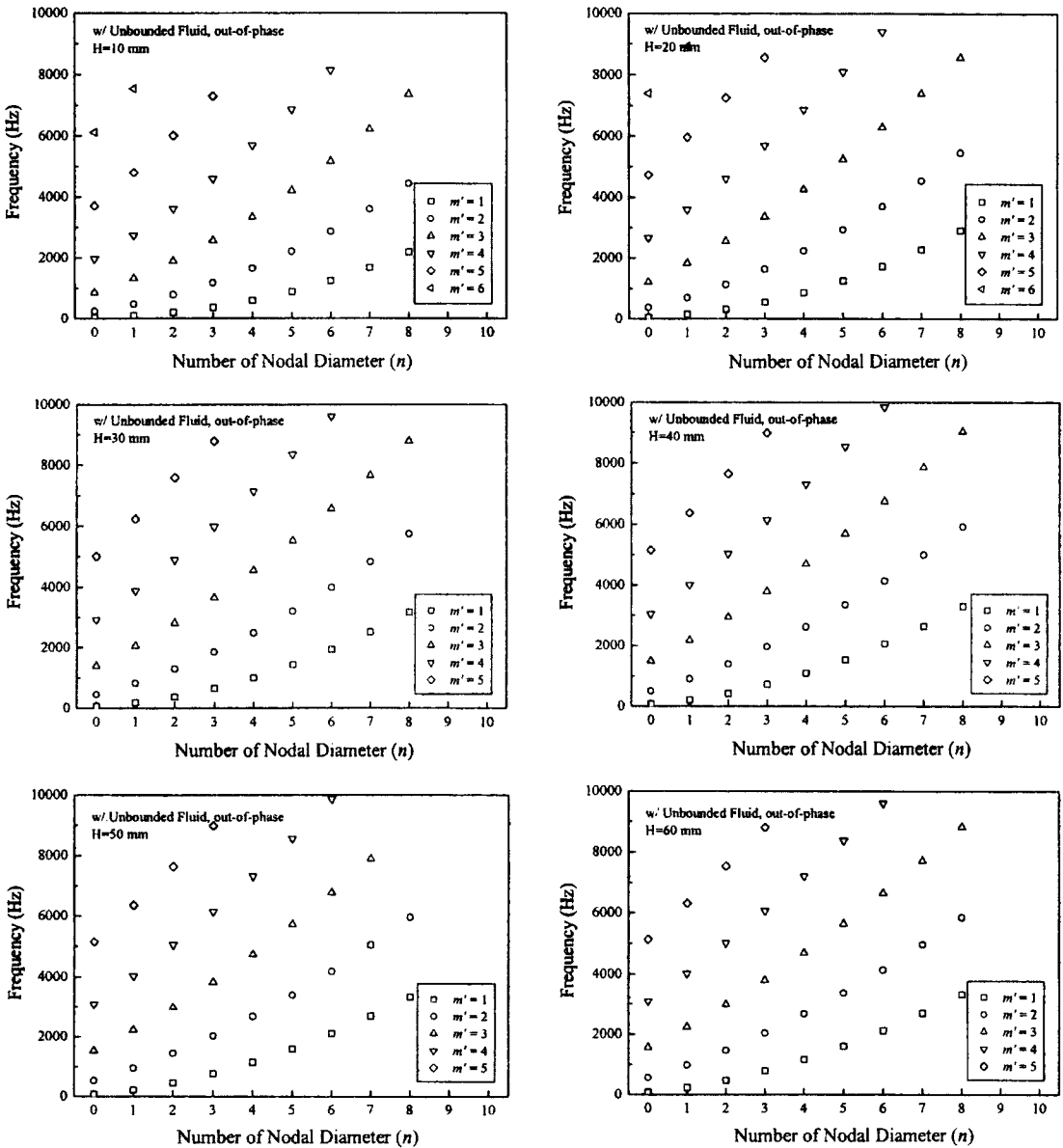


Fig. 8 Out-of-phase mode frequencies of two plates coupled with fluid

H, between the plates significantly affects on the coupled natural frequencies. The decrease of distance between the plates will enlarge the hydraulic coupling effects for the out-of-phase modes. As the distance decreases, the natural frequency of the out-of-phase mode decreases by the hydrodynamic coupling effect. However for the same situation, the natural frequency for the in-phase mode increases by reducing the amount

of fluid mass itself. This trend is maintained for all over the mode numbers.

The fluid bounding effects are shown in Figs. 13 and 14. The natural frequencies of the unbounded fluid case are higher than those of the bounded fluid case for all out-of-phase modes because the fluid is free to move radially and the added mass of the mass is reduced and eventually increase the natural frequency of the wet modes.

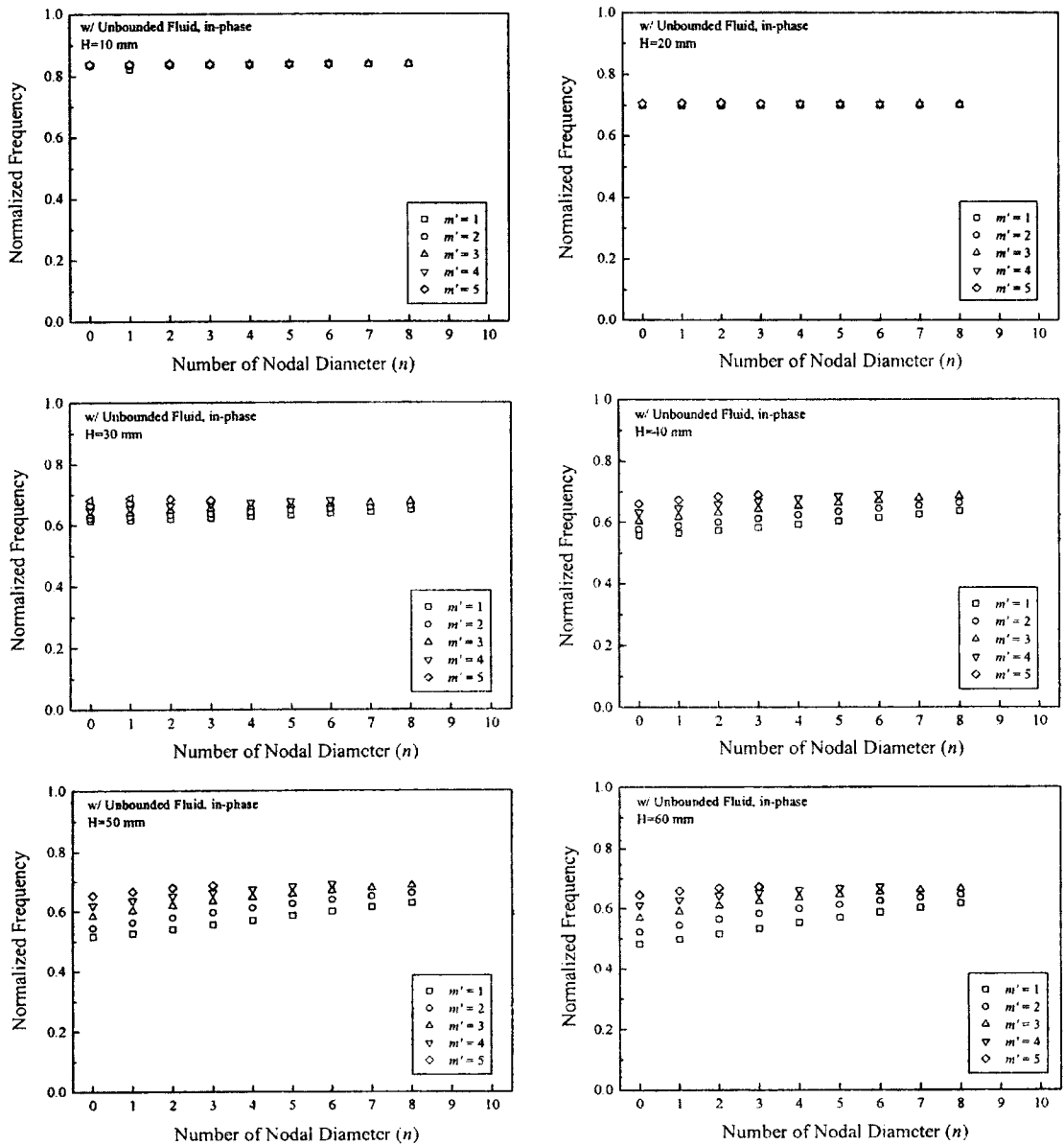


Fig. 9 Normalized frequencies of in-phase modes

However the in-phase mode natural frequencies of the unbounded fluid case are almost the same as those of the bounded fluid case because there is no fluid movement between two plates and the same amount of added mass is always conserved for the in-phase modes.

Normalized frequency comparisons between bounded and unbounded fluid cases are shown in Figs. 15 and 16, which show that in-phase mo-

des have the same fluid effect irrespective of the bounded or unbounded fluid cases but out-of-phase modes for bounded fluid case are more affected than unbounded fluid case. This can be expected from the fact that bounded fluid case has smaller frequencies than unbounded fluid case for out-of-phase modes.

The vibration characteristics summarized in this study can be used for the operator to take

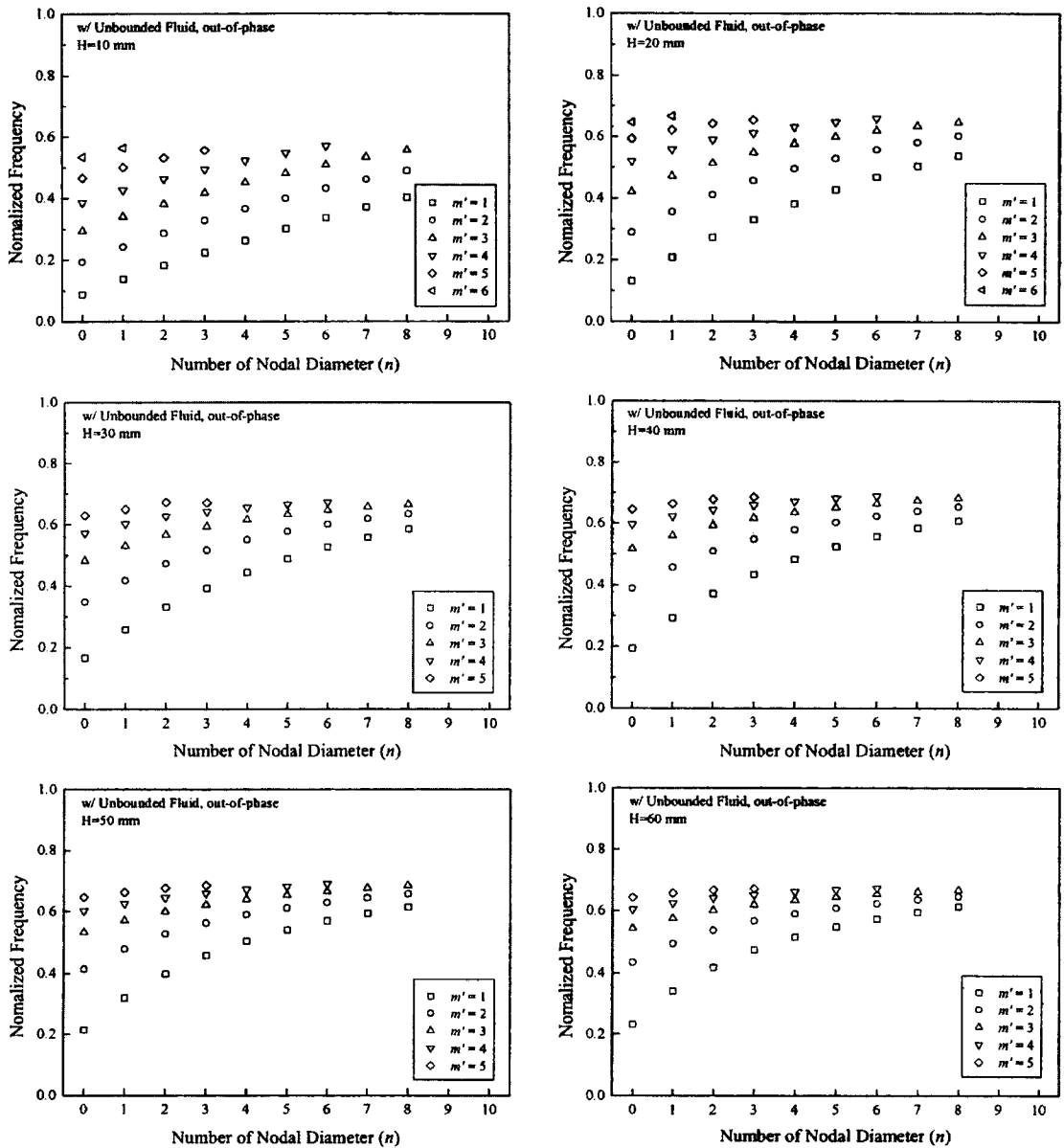


Fig. 10 Normalized frequencies of out-of-phase modes

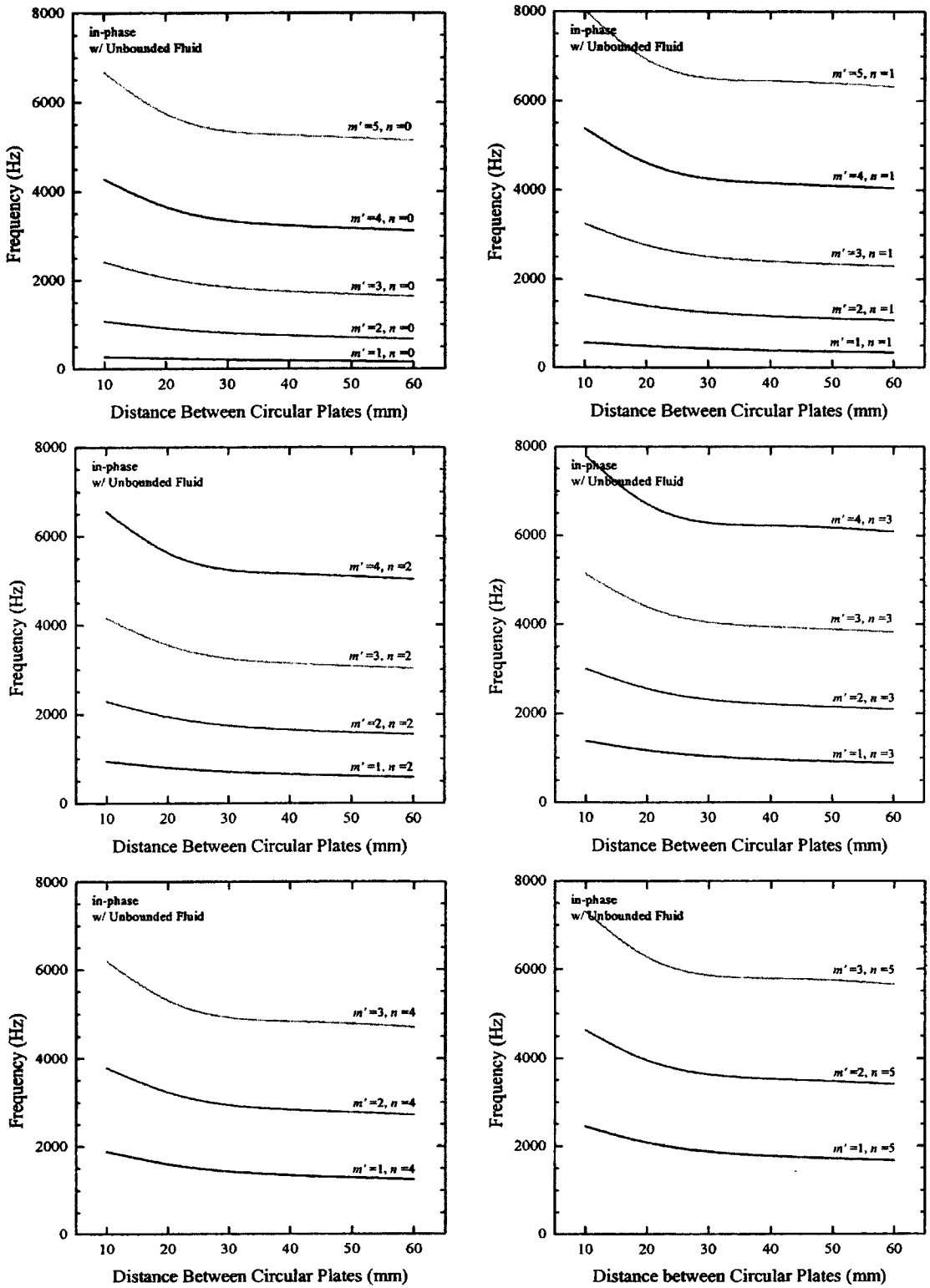


Fig. 11 Fluid gap effect on natural frequencies of in-phase modes



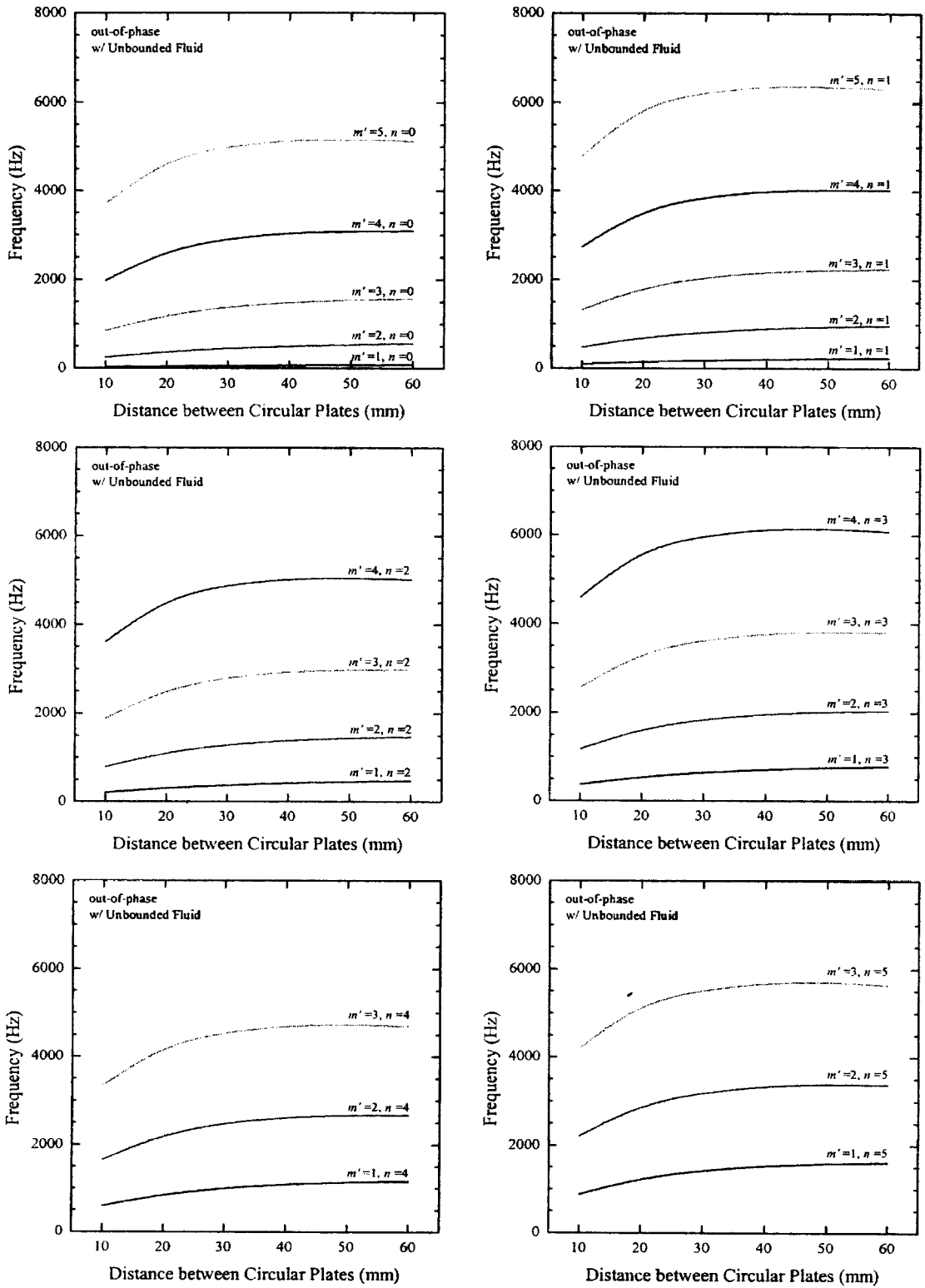


Fig. 12 Fluid gap effect on natural frequencies of out-of-phase modes

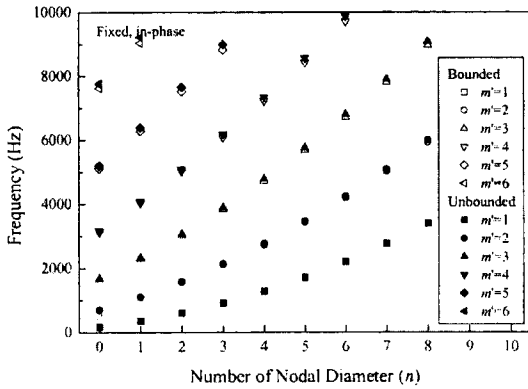


Fig. 13 Frequency comparisons of in-phase modes between bounded and unbounded fluid

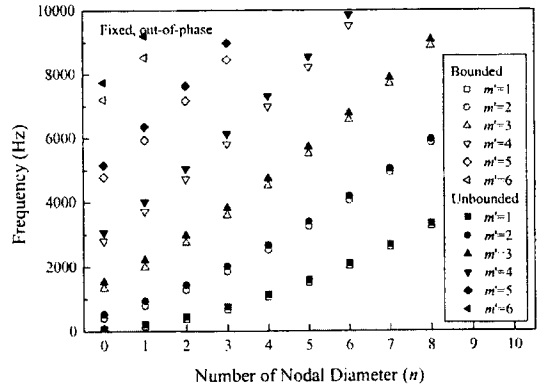


Fig. 14 Frequency comparisons of out-of-phase modes between bounded and unbounded fluid

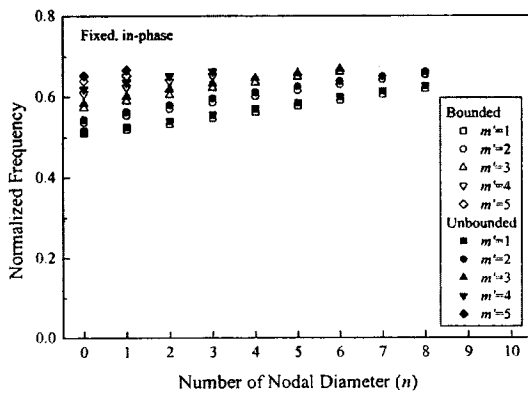


Fig. 15 Normalized frequency comparisons of in-phase modes between bounded and unbounded fluid

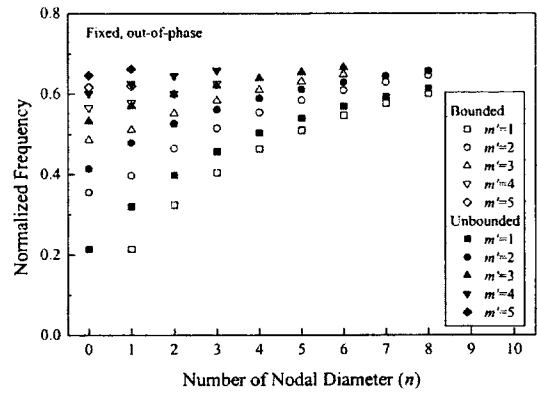


Fig. 16 Normalized frequency comparisons of out-of-phase modes between bounded and unbounded fluid

some actions to prevent damages resulting from the abnormal vibration which can be predicted from this study.

### 5. Conclusions

An analytical method to estimate the coupled frequencies of the circular plates coupled with fluid is developed using the finite Fourier-Bessel series expansion and Rayleigh-Ritz method. To verify the validity of the analytical method developed, finite element method is used and the frequency comparisons between them are found to be in good agreement. The effect of the fluid bounding and distance between plates on the frequencies is investigated generating following

conclusions ;

- (1) The out-of-phase and in-phase modes are observed alternately when the number of nodal circles increases for the fixed nodal diameter.
- (2) The effect of the contained fluid on the plate frequencies is found to be more severe in out-of-phase modes than in-phase modes. Especially as number of diametrical and circular modes decrease, the effect is more significant.
- (3) The decrease of distance between the plates results in an increase in the in-phase modes and a decrease in the out-of-phase modes. An increase in the number of diametrical and circular modes shows a monotonic increase in the normalized natural frequencies.
- (4) The frequencies of unbounded fluid case

are almost the same as those of bounded case for the in-phase modes. But the frequencies of unbounded fluid case are higher than those of bounded case for the out-of-phase modes.

(5) The fluid contained between two plates generates the same trend irrespective of the bounded or unbounded fluid cases.

### References

- Amabili, M., Frosali, G. and Kwak, M. K., 1996, "Free Vibrations of Annular Plates Coupled with Fluids," *Journal of Sound and Vibration*, Vol. 91, pp. 825~846.
- ANSYS, 2001, *ANSYS Structural Analysis Guide*, ANSYS, Inc., Houston.
- Bauer, H. F., 1995, "Coupled Frequencies of a Liquid in a Circular Cylindrical Container with Elastic Liquid Surface Cover," *Journal of Sound and Vibration*, Vol. 180, pp. 689~694.
- Chiba, M., 1994, "Axisymmetric Free Hydroelastic Vibration of a Flexural Bottom Plate in a Cylindrical Tank Supported on an Elastic Foundation," *Journal of Sound and Vibration*, Vol. 169, pp. 387~394.
- De Santo, D. F., 1981, "Added Mass and Hydrodynamic Damping of Perforated Plates Vibrating in Water," *Transaction of the ASME, Journal of Pressure Vessel Technology*, Vol. 103, pp. 175~182.
- Hagedorn, P., 1994, "A Note on the Vibrations of Infinite Elastic Plates in Contact with Water," *Journal of Sound and Vibration*, Vol. 175, pp. 233~240.
- Jhung, M. J., Jeong, K. H. and Hwang, W. G., 2002, "Modal Analysis of Eccentric Shells with Fluid-Filled Annulus," *Structural Engineering and Mechanics*, Vol. 14, No. 1, pp. 1~20.
- Kwak, M. K., 1991, "Vibration of Circular Plates in Contact with Water," *Transaction of the ASME, Journal of Applied Mechanics*, Vol. 58, pp. 480~483.
- Kwak, M. K. and Kim, K. C., 1991, "Axisymmetric Vibration of Circular Plates in Contact with Fluid," *Journal of Sound and Vibration*, Vol. 146, pp. 381~389.
- Montero de Espinosa, F. and Gallego-Juarez, J. A., 1984, "On the Resonance Frequencies of Water-Loaded Circular Plate," *Journal of Sound and Vibration*, Vol. 94, pp. 217~222.
- Sneddon, Ian N., 1951, *Fourier Transforms*, McGraw-Hill, New York.